CHEMISTRY
A EUROPEAN JOURNAL

ChemPubSoc
Europe

DOI: 10.1002/chem.201201698

Light-Driven Coordination-Induced Spin-State Switching: Rational Design of Photodissociable Ligands

Steffen Thies,[a] Hanno Sell,[a] Claudia Bornholdt,[a] Christian Schütt,[a] Felix Köhler,[a] Felix Tuczek,[b] and Rainer Herges*[a]

Dedicated to G. A. Olah on the occasion of his 85th birthday

Abstract: The bistability of spin states (e.g., spin crossover) in bulk materials is well investigated and understood. We recently extended spin-state switching to isolated molecules at room temperature (light-driven coordination-induced spin-state switching, or LD-CISSS). Whereas bistability and hysteresis in conventional spin-crossover materials are caused by cooperative effects in the crystal lattice, spin switching in LD-CISSS is achieved by reversibly changing the coordination number of a metal complex by means of a photochromic ligand that binds in one configuration but dissociates in the other form. We present mathematical proof that the maximum efficiency in property switching by such a photodissociable ligand (PDL) is only dependent on the ratio of the association constants of both configurations. Rational design by using DFT calculations was applied to develop a photoswitchable ligand with a high switching efficiency. The starting point was a nickel–porphyrin as the transition-metal complex and 3-phenylazopyridine as the photodissociable ligand. Calculations and experiments were performed in two iterative steps to find a substitution pattern at the phenylazopyridine ligand that provided optimum performance. Following this strategy, we synthesized an improved photodissociable ligand that binds to the Ni–porphyrin with an association constant that is 5.36 times higher in its *trans* form than in the *cis* form. The switching efficiency between the diamagnetic and paramagnetic state is efficient as well (72% paramagnetic Ni–porphyrin after irradiation at 365 nm, 32% paramagnetic species after irradiation at 440 nm). Potential applications arise from the fact that the LD-CISSS approach for the first time allows reversible switching of the magnetic susceptibility of a homogeneous solution. Photoswitchable contrast agents for magnetic resonance imaging and light-controlled magnetic levitation are conceivable applications.

Keywords: coordination number · nickel · photochromism · porphyrinoids · spin crossover

Introduction

Magnetic bistability due to the orientation of magnetization in ferromagnetic materials or spin-state bistability based on spin crossover in transition-metal complexes are typical solid-state phenomena. The reason for the hysteresis is the cooperative interaction between a large number of spin centers.[1] In isolated molecules, bistability is therefore observed only at low temperatures.[2] Switching between two stable/metastable spin states in isolated molecules at room temperature, however, would open a number of new applications in the field of switchable contrast agents for magnetic resonance imaging (MRI),[36] light-controlled diamagnetic levitation,[7,8] data storage, or spintronics.[9] Probably the first approach to spin-state switching that is not based on cooperative effects of neighboring spin centers was proposed by Boillot and Zarembowitch et al.[10–13] They chose Fe^{II} as the transition-metal ion in conjunction with ligands that isomerize upon irradiation and concomitantly change their ligand field strength, which leads to a change in magnetic properties (light-driven ligand-induced spin change, or LD-LISC). Another approach is based on changing the spin state by changing the oxidation state of the transition-metal ion. Again the switchable redox behavior of photochromic ligands is used to change the oxidation state and concomitantly the spin state of the transition-metal ion.[14,15] However, the effects in both systems are weak and reversibility was restricted to only a few cycles.[16]

We recently developed the light-driven coordination-induced spin-state switching (LD-CISSS) approach.[17–19] In contrast to conventional spin-crossover complexes, LD-CISSS systems are bistable over a very large temperature

[a] Dr. S. Thies, H. Sell, Dr. C. Bornholdt, C. Schütt, Dr. F. Köhler, Prof. Dr. R. Herges
Institut für Organische Chemie, Universität Kiel
Otto-Hahn-Platz 4, 24118 Kiel (Germany)
Fax: (+49) 431-880-1558
E-mail: rherges@oc.uni-kiel.de

[b] Prof. Dr. F. Tuczek
Institut für Anorganische Chemie, Universität Kiel
Max-Eyth-Strasse 2, 24118 Kiel (Germany)

Supporting information for this article is available on the WWW under http://dx.doi.org/10.1002/chem.201201698. It includes UV/Vis spectra, extinction coefficients, half-lives of thermal isomerization, a complete list of association constants, the numbering of the structures for the assignment of the NMR spectroscopic signals, and the computational details of the DFT calculations.

range (from the melting point of the solvent to well above room temperature), they are air stable, completely fatigue resistant, and most importantly they are bistable in homogeneous solution. The idea is based on the fact that a number of transition metals in some oxidation states (e.g., Mn^{III}, Fe^{II}, Fe^{III}, Co^{II}, Co^{III}, and Ni^{II}) can exist in two or three different spin states depending on their coordination number. We chose Ni^{II} because it is stable in its oxidation state in air (which facilitates synthesis and handling), and the spin states are reliably predicted by quantum chemical calculations (which makes the molecules easier to design). Both aspects are distinct advantages over Fe^{II}, which is most frequently used in spin-crossover experiments. The benefits more than outweigh the disadvantage that the attainable spin change is smaller in Ni^{II} ($\Delta S=1$) than in Fe^{II} ($\Delta S=2$). Square-planar Ni^{II} complexes (coordination number $n=4$) are always diamagnetic, and square-pyramidal ($n=5$) as well as octahedral ($n=6$) complexes are paramagnetic ($S=1$).[20] The change in spin state of Ni^{II} is due to a change in occupancy of the $d_{x^2-y^2}$ and d_{z^2} orbitals. In square-planar Ni^{II} complexes, the d_{z^2} orbital is doubly occupied, and $d_{x^2-y^2}$ is empty (Figure 1, left, Ni porphyrin). Axial donor ligands increase the energy of the d_{z^2} MO close to the level of the empty $d_{x^2-y^2}$ orbital (Figure 1, Ni porphyrin with one axial pyridine, singlet). In electron-poor square-planar complexes, the approach of a single, strong donor ligand is sufficient to induce spin crossover, thus leading to a triplet high-spin complex with one electron in d_{z^2} and one in $d_{x^2-y^2}$ (Figure 1, Ni porphyrin with one pyridine ligand triplet). A second axial ligand further stabilizes the triplet high-spin state (Figure 1, Ni porphyrin with two axial pyridine ligands).

A change in coordination number from $n=4$ to $n=5$ (or to $n=6$), therefore, gives rise to a change in spin state from $S=0$ to $S=1$. To put this concept into operation, we chose porphyrins as platforms ($n=4$) and photochromic molecules as axial ligands to change the coordination number. Porphyrins have a distinct advantage over other square-planar complexes coordinated by, for example, cyclam or salen ligands, in that they are more rigid, and therefore would not (or only slightly) deform upon axial coordination or decoordination.

Two approaches were pursued to put the light-driven axial coordination/decoordination into practice: 1) the "record player" design with the photoswitchable ligand covalently tethered to the porphyrin,[19,21] and 2) the photodissociable ligand (PDL) approach, which is based on switchable steric hindrance (Figure 2).[18] Both strategies have pros and cons. Record-player molecules, if properly designed, have higher switching efficiencies; however, they undergo intermolecular coordination at high concentrations. PDL-based systems do not suffer from the latter restriction; however, a large excess amount of the photoswitchable ligand is needed at low concentrations. In a preceding study, we used

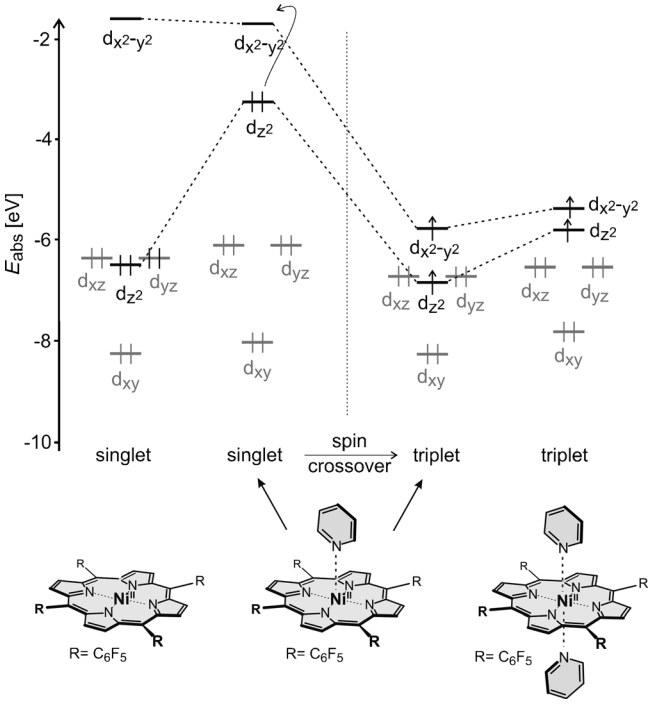

Figure 1. Molecular orbital scheme depicting the electronic structure of 4-coordinate, square-planar Ni^{II} in the singlet state (low spin); 5-coordinate, square-pyramidal Ni^{II} in the singlet state (low spin) and in the triplet state (high spin); and 6-coordinate square-bipyramidal Ni^{II} in the triplet state (high spin). Orbital energies (E_{abs}) are given in eV and are calculated from Ni–tetrakis(pentafluorophenyl)porphyrin **1** and pyridine at the B3LYP/6-31G* level of DFT. For further details, see the Supporting Information.

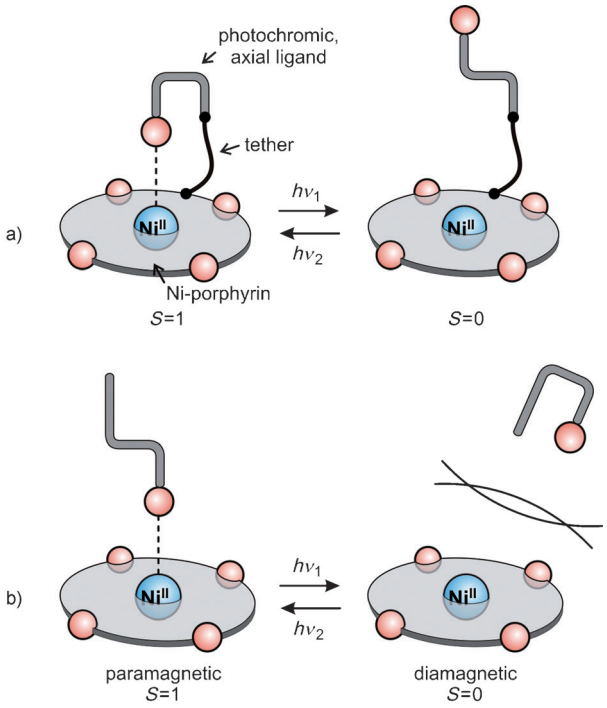

Figure 2. Two approaches to the light-driven, coordination-induced spin-state switching (LD-CISSS): a) the "record player" design and b) photodissociable ligand (PDL) strategy.

symmetric azopyridines as PDLs. Since azopyridines contain two coordinating pyridine rings, they form coordination polymers with porphyrins that precipitate at high concentrations.[18] Therefore, we set out to design phenylazopyridines with only one coordination site that would still operate at high concentrations. Consequently, large changes in the magnetic susceptibility of homogeneous solutions could be obtained, which are important for applications such as light-controlled magnetic levitation. So far, no method other than LD-CISSS has the potential to achieve that.

Results and Discussion

General considerations: The photodissociable ligand (PDL) approach can be used to control any property that depends on the coordination[22–25] or preferentially on the coordination number of a metal complex. The maximum change in a property that can be obtained in such a system is achieved if one were able to switch the coordination of the photodissociable ligand between complete binding and no binding at all. In the present case, this would correspond to changing all Ni ions in solution between diamagnetic and paramagnetic. If we assume the following coordination equilibria (only 1:1 complexes are formed) [Eq. (1)]:

$$\begin{aligned} &P + \mathbf{L}_a \overset{K_a}{\rightleftharpoons} P\mathbf{L}_a \\ &P + \mathbf{L}_b \overset{K_b}{\rightleftharpoons} P\mathbf{L}_b \end{aligned} \tag{1}$$

in which P is the porphyrin (or other metal-base complex), $\mathbf{L}_a$ is the ligand in configuration a, and $\mathbf{L}_b$ is the ligand in configuration b. The switching efficiency (SE) [%] can be defined as [Eq. (2)]:

$$SE = 100\left(\frac{[PL_a] - [PL_b]}{[P]_{tot}}\right) \tag{2}$$

in which $[P\mathbf{L}_a]$ is the concentration of complex $P\mathbf{L}_a$, $[P\mathbf{L}_b]$ is the concentration of complex $P\mathbf{L}_b$, and $[P]_{tot}$ is the total concentration of P.

In practice, at low concentrations of P and low association constants, a large excess amount of the ligand is needed to enforce complexation. We therefore set $[\mathbf{L}]_{tot} = [\mathbf{L}]$ and $[P]_{tot} = [P] + K_a[\mathbf{L}][P]$, and determined the concentration of free P and of the complex P**L** as [Eq. (3)]:

$$[P] = \frac{[P]_{tot}}{1 + K[L]_{tot}} \text{ and } [PL] = \frac{K[P]_{tot}[L]_{tot}}{1 + K[L]_{tot}} \tag{3}$$

The switching efficiency can now be expressed as a function of the total ligand concentration ($[\mathbf{L}]_{tot}$) and the association constants (K_a, K_b), since $[P]_{tot}$ cancels out [Eq. (4)]:

$$SE = 100\frac{[L]_{tot}(K_a - K_b)}{(1 + K_a[L]_{tot})(1 + K_b[L]_{tot})} \tag{4}$$

In practice, it is particularly interesting to know which ligand concentration would lead to a maximum switching efficiency SE_{max}. The optimal ligand concentration $[\mathbf{L}]_{opt}$ is obtained by partial differentiation of SE with respect to $[\mathbf{L}]_{tot}$ [Eq. (5)]:

$$[L]_{opt} = \frac{1}{\sqrt{K_a K_b}} \tag{5}$$

Surprisingly, $[\mathbf{L}]_{opt}$ is independent of the porphyrin concentration [P] as long as there is a large molar excess amount of the ligand in solution ($[\mathbf{L}]_{tot} \approx [\mathbf{L}]$). The maximum switching efficiency (SE_{max}) [%] is obtained by substitution of $[\mathbf{L}]_{tot}$ for $[\mathbf{L}]_{opt}$ in Equation (4) [Eq. (6)]:

$$SE_{max} = 100\frac{1 - \sqrt{K_b/K_a}}{1 + \sqrt{K_b/K_a}} \tag{6}$$

SE_{max} only depends on the ratio of the association constants of the photodissociable ligand (PDL) in both switching states. For the design of an efficient PDL, it is important to note that the switching efficiency is 100% if K_b is zero, independent of the association constant K_a. Therefore, it is probably a reasonable strategy to put more emphasis within ligand design to prevent the ligand in its conformation b ($\mathbf{L}_b$) from binding, rather than to optimize the binding properties of conformation a ($\mathbf{L}_a$).

The optimal ligand concentration ($[\mathbf{L}]_{opt}$) and the maximum switching efficiency (SE_{max}) are system parameters that characterize the performance of a photodissociable ligand with a given transition-metal complex. Equally important in affecting the switching efficiency are the photostationary states (PSS_1 and PSS_2) of the PDL upon irradiation with light of wavelengths $h\nu_1$ and $h\nu_2$ [Eq. (7)]:

$$\begin{aligned} &\mathbf{L}_a \underset{h\nu_2}{\overset{h\nu_1}{\rightleftharpoons}} \mathbf{L}_b \\ &h\nu_1 : PSS_1 = \frac{[L]_b}{[L]_a + [L]_b} \\ &h\nu_2 : PSS_2 = \frac{[L]_b}{[L]_a + [L]_b} \end{aligned} \tag{7}$$

Incomplete conversion of the ligand from one configuration to the other can be accounted for by setting up pseudo association constants K'_a and K'_b as linear combinations of K_a and K_b weighted by the photostationary states PSS_1 and PSS_2 [Eq. (8)]:

$$\begin{aligned} K'_a &= (1 - PSS_2)K_a + PSS_2 K_b \\ K'_b &= (1 - PSS_1)K_a + PSS_1 K_b \end{aligned} \tag{8}$$

From substitution of K_a and K_b by K'_a and K'_b in Equations (4) and (6), we obtain $[\mathbf{L}]_{opt}$ and SE_{max} for systems with incomplete photochemical conversion. Again we draw the conclusion that an optimal PDL should exhibit a complete conversion to the nonbinding configuration. An efficient

back-isomerization to the binding isomer is less important as long as there is a large excess amount of the ligand.

At higher concentrations of the porphyrin (lower ligand to porphyrin ratios) we expect deviations from Equations (4) and (6). In these cases, nonlinear methods should be applied to determine $[\mathbf{L}]_{opt}$ and SE_{max}. For systems that include more than two complex species, that is 2:1 complexes, such as the Ni–porphyrin/phenylazopyridine system presented here, an analytical solution of the underlying mathematical problem is not possible. However, iterative solutions based on up to six association constants that describe the formation of 1:1 and 2:1 complexes demonstrate that $[\mathbf{L}]_{opt}$ and SE_{max} are still independent of the porphyrin concentration if a large excess amount of the ligand is provided (see the Experimental Section). Therefore, we consider $[\mathbf{L}]_{opt}$ and SE_{max} as defined in Equations (4) and (6) to be important parameters for ligand design and for setting up the optimal conditions for property switching with PDLs.

Ligand design: Phenylazopyridines are an appealing class of compounds to develop photodissociable ligands. They combine the switching capabilities of azobenzene with the coordination properties of pyridine. The three regioisomers, 2-, 3-, and 4-phenylazopyridine (Scheme 1), have been investigated by Otsuki et al. as ligands for the light-triggered luminescence modulation of Zn–porphyrins.[22,24] Preliminary studies in combination with Ni–porphyrins[26] revealed that 4-phenylazopyridine exhibits limited photochromic properties and a fast thermal back-isomerization, which is even further accelerated by coordination to transition-metal ions. Moreover, extremely large substituents are needed to implement sterical hindrance.[25] 2-Phenylazopyridine (alongside other 2-substituted pyridines) is a very weak ligand.[23] The *trans* configuration does not bind to Ni–porphyrins above the detection limit (UV), and association is extremely weak in the *cis* form. This is clearly due to the steric hindrance of the substituent in the 2-position.

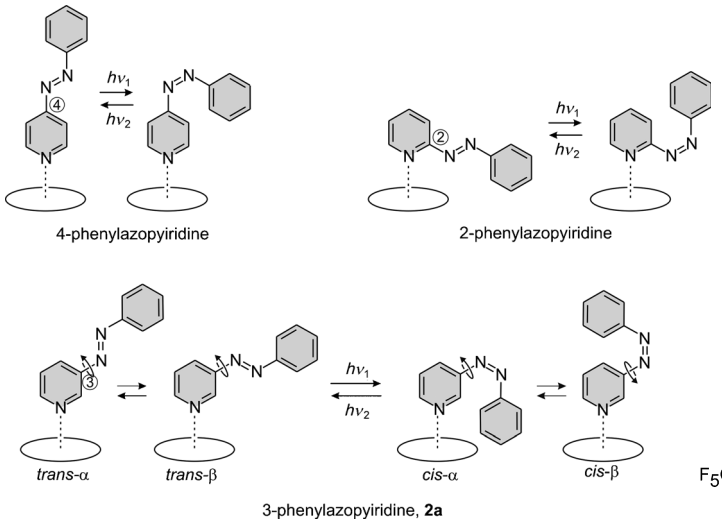

Scheme 1. Three regiosiomers of phenylazopyridine in *cis* and *trans* configurations and simplified binding modes to a square-planar platform complex (e.g., Ni–porphyrin). For 3-phenylazopyridine, the two conformations of both configurations are given (*trans*-α, *trans*-β, *cis*-α, and *cis*-β).

3-Phenylazopyridine is probably the most suitable starting point for the development of photodissociable ligands. The parent compound (similar to azobenzene) isomerizes from *trans* to *cis* upon irradiation with UV light of 365 nm. In the photostationary state (PSS-365), a mixture of 37% *trans* and 63% *cis* isomer is attained. Back-isomerization to the *cis* isomer is achieved at 440 nm (PSS-440: 80% *trans*, 29% *cis*). Heating of the photostationary equilibrium to 70° for several hours yields the pure *trans* isomer. However, the parent 3-phenlyazopyridine is not suitable as a photodissociable ligand, because it binds to Ni–porphyrin with similar association constants in the *trans* and *cis* configurations. This is due to the fact that the *trans* and the *cis* isomer each can have two conformations (*trans*-α, *trans*-β, *cis*-α, and *cis*-β; Scheme 1, bottom). Whereas both *trans* conformations (*trans*-α, *trans*-β) are able to bind, only the *cis*-α conformation experiences some steric repulsion with the porphyrin framework. The *cis*-β conformation still binds.

In our first step towards the development of a photodissociable ligand, we concentrated on disfavoring the *cis*-β conformation in such a way that only nonbinding *cis*-α would be left in the conformational equilibrium of the *cis* isomer. The most straightforward way to achieve this is to increase the steric hindrance of the pyridine and the phenyl ring by substitution with large substituents in the 4-position of the pyridine ring and/or in the 2,5-positions of the phenyl ring. *Ortho* substitution of the rings with respect to the azo group, moreover, has the advantage that light-induced *trans–cis* as well as *cis–trans* isomerization usually are more efficient than in the parent systems.[27] Seven different 4-substituted 3-phenylazopyridines (**2a–g**; Scheme 2) were synthesized and calculated at the PBE/SVP level of density functional theory.[28,29]

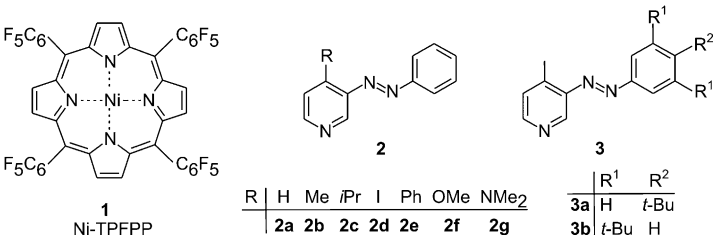

Scheme 2. Ni^{II}–tetrakis(pentafluorophenyl)porphyrin (**1**) and the 4-substituted 3-phenylazopyridines **2a–g** that were used as axial ligands. The PDLs of the second generation are substituted on the phenyl ring by *tert*-butyl substituents (**3a** and **3b**).

The calculated relative energies (Scheme 3) clearly show that large substituents in the 4-position at the pyridine ring indeed disfavor the *trans*-α and *cis*-β conformations (steric collisions are indicated in curved bold lines in Scheme 3, bottom). As a consequence, the binding *trans*-β and the non-

	R	*trans*-α	*trans*-β	*cis*-α	*cis*-β
2a	H	0.00	-0.78	0.00	0.37
2b	Me	0.00	0.90	0.00	1.94
2c	*i*Pr	0.00	2.18	0.00	2.14
2d	I	0.00	3.51	0.00	2.86
2e	Ph	0.00	3.59	0.00	0.92
2f	OMe	0.00	1.53	0.00	0.02
2g	NMe_2	0.00	2.79	0.00	3.09

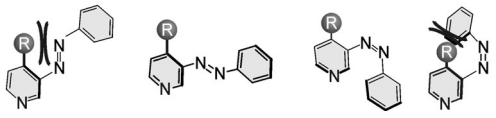

Scheme 3. DFT (PBE/SVP)-calculated energies of 4-substituted 3-phenylazopyridines **2a**–**g** in their *trans* and *cis* configurations, and their α and β conformations (*trans*-α, *trans*-β, *cis*-α, and *cis*-β). The values are in kcal mol^{-1} relative to the α conformation of each configuration. Regions of steric hindrance induced by the substituents are indicated with black curves.

binding *cis*-α forms should be the predominant species in solution, thus leading to a large discrimination of the binding affinity.

Photochemical properties of 3-azopyridines in solution: To test our hypothesis and evaluate the photochemical properties, we synthesized the 3-phenylazopyridines **2a**–**g** and determined the photostationary states for **2a**–**g** and **3b** upon irradiation at 365 and 440 nm (PSS-365 and PSS-440) in the absence of Ni–porphyrin **1**. Additionally, the thermal half-life of the *cis* isomer was determined by NMR spectroscopy[30] (see Table 1; for the UV spectra, see the Supporting Information).

Table 1. Photostationary states of 4-substituted 3-phenylazopyridines **2a**–**g** and **3b**, and thermal half-lives of their *cis* isomers in the absence of Ni–porphyrin **1**.

	R	PSS-365[a] *cis* [%]	PSS-440[b] *cis* [%]	Thermal half-life [h][c]
2a	H	63	20	228±5
2b	Me	72	17	100±2
2c	*i*Pr	75	13	316±8
2c+**1**[d]	*i*Pr	75	14	249±6
2d[e]	I	86	10	115±2
2e	Ph	84	13	206±3
2f	OMe	90	13	915±4
2g	NMe_2	66	62	31±0.5
3b	Me, 3,5-*t*Bu	91	15	370±6

[a] Percentage of the *cis* isomer in the *trans*/*cis* photostationary equilibrium (PSS) after irradiation at 365 nm in [D_8]toluene (determined by ^{1}H NMR spectroscopy). [b] Percentage of the *cis* isomer in the *trans*/*cis* photostationary equilibrium (PSS) after irradiation at 455 nm in [D_8]toluene (determined by ^{1}H NMR spectroscopy). [c] In [D_8]toluene, 25 °C (determined by ^{1}H NMR spectroscopy). [d] 105 mM **2c** and 106 μM porphyrin **1**. [e] Compound **2d** decomposed after several switching cycles.

The *cis*-isomer concentration of all azopyridines can be increased to more than 60% in the photostationary state (PSS) upon irradiation with UV light (365 nm). Compound **2d**, however, decomposes after prolonged irradiation with UV light. The corresponding reisomerization can be achieved by irradiation with visible light (440 nm) to a percentage of more than 80% *trans* in all but one case. No significant conversion could be obtained for **2g** (Table 1), probably because the n–π* and the π–π* bands have similar absorption maxima and intensity in both configurations.[23] The thermal half-lives of all *cis* compounds range from 30 to 900 h in toluene at 25 °C. Addition of the Ni–porphyrin **1** (106 μM) reduces the half-life of *cis*-**2c** (105 mM) from 316 to 249 h in [D_8]toluene at 25 °C. Thus, all 3-phenylazopyridines except **2d** and **2g** are suitable as photoswitchable compounds. However, their applicability as photodissociable ligands still has to be proven by the determination of their association constants to Ni–porphyrin **1** in *trans* (binding) and *cis* configuration (nonbinding).

Determination of association constants: Previously, we have demonstrated that the chemical shift of the pyrrol protons of the Ni–porphyrin is an excellent probe to accurately determine association constants of axial ligands.[17,18] Upon coordination of one or two axial ligands, the Ni ion changes the spin state from diamagnetic ($S=0$) to paramagnetic ($S=1$), thus leading to a very large downfield shift of the pyrrole protons from $\delta=8.54$ to 52.4 ppm. Ligand exchange is fast on the NMR spectroscopic timescale. Therefore the observed average chemical shift is an accurate measure of the ratio between dia- and paramagnetic species in solution, which was determined as reported previously.[31]

We performed ^{1}H NMR spectroscopic titration experiments with 3-phenylazopyridines **2a**–**g** and **3b**. Different amounts (10, 50, 100, 175, 350, 500, 650, 800, 1000, 1500, 2000 equiv) of the *trans*-azopyridines were added to a 106 μM solution of **1** in [D_8]toluene. The *cis* to *trans* ratio and the association constants were determined as reported previously.[18] To obtain a more accurate extrapolation to the association constants of the pure *cis* isomers we performed the NMR spectroscopic titration with three different *trans*/*cis* ratios: 1) pure *trans* isomer, 2) equilibrium at the PSS-365, and 3) approximate 1:1 ratio of *trans* and *cis* isomer (obtained from PSS-365 by partial thermal reisomerization). For the determination of the association constants it is important to note that the pure Ni–porphyrin is the only diamagnetic species in solution, whereas there are five Ni–porphyrin complexes that are paramagnetic: the porphyrin with one and two *trans* ligands, with one and two *cis* ligands, and the mixed complex with one *cis* and one *trans* ligand. Hence there are six association constants that have to be determined for each ligand (i.e., 56 association constants in total). For each ligand, 10 titration points at three different *cis*/*trans* ratios were determined (i.e., in total, 240 NMR spectra were recorded). The association constants were calculated by using a nonlinear titration curve fitting.[17,32,33] The most important data to prove our concept of photodissociation by switching of the steric hindrance are the association constants of the 1:1 and 1:2 complexes of the porphyrin with the *trans* and the *cis* ligands (see Table 2; for a com-

Table 2. Association constants of porphyrin **1** with azopyridine derivates **2a–f** and **3b** at 298 K in [D_8]toluene, given in $L\,mol^{-1}$ (1:1 complexes) and $L^2\,mol^{-2}$ (1:2 complexes). For a definition of the association constants (P: **1**; **L**: **2a–f**, **3b**), see the footnote.[a]

	2a	**2b**	**2c**	**2d**	**2e**	**2f**	**2g**[b]	**3b**
$K_{1,trans}$	2.80	5.83	4.90	0.81	3.14	9.49	55.3	6.27
$K_{1,cis}$	1.02	2.84	1.96	0.36	2.29	6.99		1.17
ratio[c]	2.75	2.05	2.50	2.25	1.37	1.36		5.36
$K_{2,trans}$	17.0	17.0	13.6	10.1	14.0	18.7	18.7	14.2
$K_{2,cis}$	28.9	8.64	9.38	6.99	18.0	31.7		4.93
ratio[c]	0.59	1.97	1.45	1.44	0.77	0.59		2.88

[a] $K_{1,trans} = P + \mathbf{L}_{trans} \rightarrow P{\cdot}\mathbf{L}_{trans}$; $K_{1,cis} = P + \mathbf{L}_{cis} \rightarrow P{\cdot}\mathbf{L}_{cis}$; $K_{2,trans} = P{\cdot}\mathbf{L}_{trans} + \mathbf{L}_{trans} \rightarrow P{\cdot}(\mathbf{L}_{trans})_2$; $K_{2,cis} = P{\cdot}\mathbf{L}_{cis} + \mathbf{L}_{cis} \rightarrow P{\cdot}(\mathbf{L}_{cis})_2$. A full list of all association constants is given in the Supporting Information. [b] $K_{1,cis}$ and $K_{2,cis}$ of **2g** could not be determined because of inefficient photochemical conversion from *trans* to *cis*. [c] The ratios of the association constants between the *cis* and *trans* isomers are a measure of the switching efficiencies [see Eq. (6)].

plete list of all 56 association constants, see the Supporting Information).

The 1:1 association constants of the *trans* ligands ($K_{1,trans}$) follow the expected trend (Table 2). Donor substituents at the 4-position of the pyridine ring increase the binding strength. Most efficient is the NMe_2 group, which increases binding by a factor of 20 over the parent system. As stated in Equation (6), the maximum switching efficiency (SE_{max}) depends on the ratio of the association constants of the *trans* and the *cis* ligand (K_{trans}/K_{cis}) (Table 2). Surprisingly, increasing the steric hindrance at the 4-position does not improve the switching efficiency systematically. The parent system **2a** with a ratio $K_{trans}/K_{cis} = 2.75$ is more efficient than the methyl-substituted system **2b** (2.05) or even the isopropyl system **2c** (2.50). The 1:2 association constants ($K_{2,trans}$, $K_{2,cis}$) follow the previously observed trend.[17] K_2 generally is larger than K_1. In contrast to K_1, donor substituents at the 4-position of the pyridine ring have little effect on K_2. In the case of the very strong donor ligand **2g** ($R = NMe_2$), K_1 is larger than K_2.

In addition to the association constants of the *trans* and *cis* isomers, we also quantified the photochemically induced conversions of ligands **2a–g** in the presence of **1** and the change in magnetic properties of the solution upon irradiation at 365 (PSS-365) and 440 nm (PSS-440) (see Table 3). In all experiments, the concentration of the Ni–porphyrin was 0.106 mM. The optimal concentrations of the ligands $[\mathbf{L}]_{opt}$ were calculated from the association constants (see Table 2 and the Supporting Information) by using a nonlinear approximation. The photostationary states (PSS-365 and PSS-440) are moderate for the parent system (64 and 21% *cis*) and quite close to the values determined in the absence of the porphyrin (63 and 20% *cis*, Table 1). Photochemical conversion is increasingly efficient as the size of the substituent R in the 4-position of the pyridine ring increases (72 and 17% *cis* for R = Me, 75 and 14% for R = *i*Pr). The reason for this trend becomes clear upon close inspection of the UV/Vis spectra (see the Supporting Information). The extinction coefficient of the n–π* band ($\lambda_{max} \approx 440$ nm) of the *cis* isomer increases as the size of the substituent R increases, because the distortion from planarity of the phenylazopyridine system increases, and thus the transition is "less forbidden". Overall, however, the change in binding of the ligands upon isomerization is quite low and insufficient for an efficient switching of magnetic properties. Among the stable and reversible systems, **2c** exhibits the highest switching efficiency of only about 15%.

Theoretical calculations: To elucidate the reasons for the lack of discrimination of our PDLs in bonding to the metal, we performed further model calculations including those for the Ni–porphyrin. To save computer time, the pentafluorophenyl substituents at the porphyrin were omitted, and PBE/SVP calculations were performed to predict the energy of complex formation (ΔE_f) of the *trans*-α, *trans*-β, *cis*-α, and *cis*-β forms of the ligands **2a**, **2b**, **2c**, and **2f** with unsubstituted Ni–porphyrins.

The calculated complex formation energies (ΔE_f; Scheme 4) reveal that the parent system **2a** is the only ligand that preferentially binds in its *trans*-α conformation. As the size of the substituent R in the 4-position increases, the *trans*-α conformation is disfavored because of the steric interaction of R with the azo group. Another important and surprising conclusion that can be drawn from the calcula-

Table 3. Photochemical and magnetic switching properties of the Ni–porphyrin/phenylazopyridine systems (**1**/**2a–g**) at the photostationary states PSS-365 and PSS-440. A concentration of 0.106 mM **1** in [D_8]toluene at 25 °C was used in all experiments.

	% *cis* isomer[a]		% paramagnetic Ni^{2+}[b]		$[\mathbf{L}]_{opt}$	SE_{max}[d]	$\mathbf{L}_{exptl}$	SE_{exptl}[d]
	PSS-365	PSS-440	PSS-365	PSS-440	[equiv][c]		[equiv][e]	
2a	64	21	28.2	35.9	1230	7.3	1000	7.7
2b	72	17	44.7	55.6	902	11.2	800	10.9
2c	75	14	40.8	55.7	1175	15.2	1000	14.9
2d	81	10	decomp	decomp	3939	19.1	2000	n.d.
2e	84	13	36.3	39.0	862	2.7	800	2.7
2f	90	23	18.4	19.6	182	1.4	175	1.2
2g	63	62	91.0	90.4	n.d.	n.d.	1000	0.6
3b	91	15	71.9	31.8	1586	40.8	1500	40.1

[a] Determined by ^1H NMR spectroscopy. [b] Determined from the ^1H NMR spectroscopic shifts of the pyrrole protons.[18] [c] Theoretically calculated optimal ligand concentration in equivalents with respect to **1**. [d] The experimental values of the switching efficiencies (SE_{exptl}) are compared with theoretically calculated maximum switching efficiencies (SE_{max}) determined from the binding constants from Table 2 and the Supporting Information. [e] Ligand concentration used in the experiment.

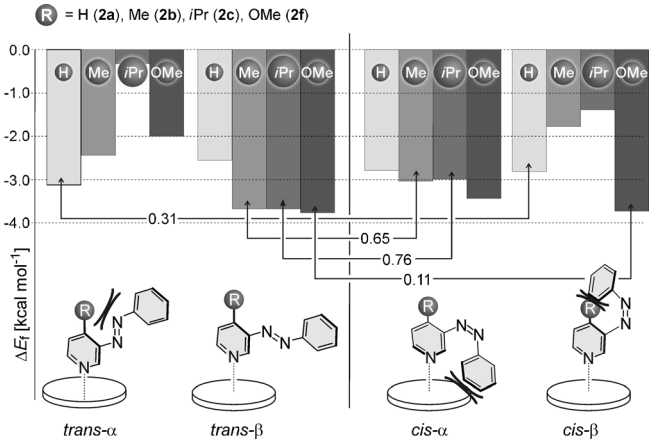

Scheme 4. DFT (PBE/SVP)-computed complex formation energies (ΔE_f) of the complexes of phenylazopyridines **2a–c** and **2f** with parent Ni–porphyrin. ΔE_f is defined as the energy that is released upon formation of the complexes (structures at the bottom) starting from the most stable conformation of each configuration. The pentafluorophenyl substituents at the porphyrin *meta* positions were omitted to save computational cost. The energy differences between the strongest binding *trans* conformation and the strongest binding *cis* conformation of each ligand are indicated by the arrows [kcal mol^{-1}].

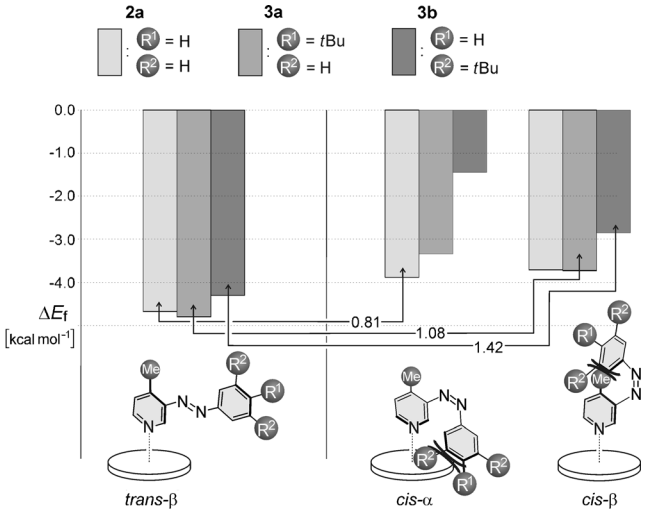

Scheme 5. Computed complex formation energies ΔE_f (PBE/TZVP//B3LYP/TZVP) including a complete basis-set extrapolation (see the Supporting Information) of **2b**, **3a**, and **3b** with Ni–TPFPP (**1**).

Table 4. Complex formation energies (ΔE_f) of **2a**, **3a**, and **3b** with Ni–porphyrin **1** calculated at the PBE/TZVP//PBE/∞ZVP level of theory.

	ΔE_f [kcal mol^{-1}] of **1** with ligand				$\Delta\Delta E_f$[a]
	trans-α	*trans*-β	*cis*-α	*cis*-β	
2a	−4.24	−4.68	−3.87	−3.72	0.81
3a	−4.28	−4.81	−3.34	−3.73	1.08
3b	−3.84	−4.29	−1.45	−2.87	1.42

[a] Energy difference between ΔE_f of the most stable *cis* and the most stable *trans* complex.

tions is the fact that the *cis*-α conformations still bind to the Ni–porphyrin quite well, and that the steric repulsion between the phenyl ring and the porphyrin is less severe than initially assumed from simple model considerations. However, the *cis*-β conformations follow the intended trend. This conformation is strongly disfavored with increasing size of the substituent R (Scheme 4). From these results we conclude that the methyl- and isopropyl-substituted systems **2b** and **2c** are good starting points for further improvement of the switching efficiency. However, to achieve this goal, the *cis*-α conformation has to be modified to prevent it from binding to the porphyrin. Thus, either steric crowding at the porphyrin unit or at the ligand has to be increased. Unfortunately, the pentafluorophenyl substituents at the *meso* positions of the porphyrin cannot be easily replaced by larger groups (e.g., mesityl) because electron-withdrawing substituents are required for effective spin switching. The most straightforward strategy is to increase steric hindrance at the phenyl ring of the ligand. To find an optimal candidate and to gain insight into the steric interactions we performed further theoretical calculations. At the phenyl ring of our ligands, substitution at the *ortho*, *meta*, or *para* position could provide additional steric repulsion. *Ortho* substitution is difficult to achieve synthetically. Therefore, we considered *t*Bu substituents in the *meta* and *para* position for preliminary model calculations (Scheme 5, Table 4).

All calculations were performed with the TURBOMOLE program.[34] The structures were optimized at the Perdew–Burke–Ernzerhof (PBE)/TZVP level of density functional theory. Single-point energy calculations were performed at the PBE-optimized geometries at the B3LYP/TZVP level. This combination of functionals and the basis set proved to provide quite accurate binding energies in Ni–porphyrins with 4-substituted pyridines in previous studies.[17] Even with the large TZVP basis set, a considerable basis set superposition error (BSSE) can be expected upon calculation of the binding energy from the separate components, thus leading to an overestimation of the complex formation energy. Unfortunately, the usual counterpoise method[35,36] cannot be applied to account for this error because the Ni^{2+} changes spin state upon complex formation from singlet to triplet. Therefore, we performed a complete basis set extrapolation according to the Helgaker scheme[37] to account for the BSSE (see the Supporting Information). At this level of theory, quite accurate complex formation energies can be expected (Table 4).

The calculated complex formation energies (ΔE_f) confirm the expected fact that neither the large *t*Bu substituent in the *para* position of the phenyl ring in **3a**, nor the two *t*Bu substituents in the *meta* position in **3b** affect the complex formation of the *trans*-β conformation. Binding of the *cis*-α conformation, however, is strongly disfavored by the two *t*Bu groups in the *meta* position in **3b**. A single *t*Bu group in the *para* position (**3a**) is considerably less effective in this respect. Moreover, the *t*Bu groups in **3b** also lower the binding strength of the *cis*-β conformation by steric interaction with the methyl group at the pyridine ring. We therefore chose **3b** as the target molecule for the synthesis of an im-

proved photodissociable ligand. Compound **3b** was prepared by the oxidation of 3,5-di-*tert*-butylaniline to the corresponding nitroso compound, and subsequent condensation with 3-amino-4-methylpyridine (for details, see the Experimental Section).

Switching experiments with improved PDL 3b: To check the success of our design, we performed photochemical switching experiments with solutions of **1** ($[\mathbf{1}]_{total}=0.106$ mM) in the presence of the optimized PDL **3b** (159 mM) in [D_8]toluene at 25 °C, and compared the switching efficiency with the parent system **2a** (130 mM). The samples were irradiated in an alternate sequence using light-emitting diodes with wavelengths of 365 (Nichia NC4U133) and 440 nm (Roithner VL-440-EMITTER) in an NMR spectroscopy tube until the PSS was reached. Figure 3 shows that the

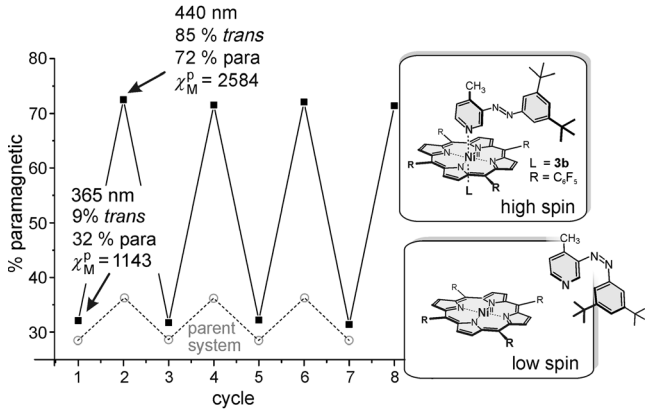

Figure 3. Reversible switching of the spin state of **1** in solution ($[\mathbf{1}]_{tot}=0.106$ mM) in the presence of an excess amount of azopyridine **3b** (159 mM) in [D_8]toluene at 25 °C by alternate irradiation with 365 and 440 nm. The molar magnetic susceptibility of the solution χ_M^P is given in 10^{-6} $cm^3 mol^{-1}$. The predominant species at both photostationary states are given on the right. The corresponding values of the less-efficient parent system (ligand **2a**) are indicated in gray.

switching process is fully reversible and does not show any fatigue. Upon irradiation with UV light at 365 nm, 91 % conversion of **3b** to the *cis* isomer is achieved. At this photostationary state, 32 % of the Ni ions in solution are paramagnetic. This corresponds to a molar magnetic susceptibility of $\chi_M^P=1143\times10^{-6}$ $cm^3 mol^{-1}$. Irradiation at 440 nm leads to a photostationary state with 15 % *cis* and 85 % *trans* isomer. Of the Ni species, 72 % are paramagnetic, and the solution attains a molar magnetic susceptibility of $\chi_M^P=2584\times10^{-6}$ $cm^3 mol^{-1}$. Hence the magnetic susceptibility of the solution can be switched by a factor of more than two! The experimentally determined switching efficiency (SE_{exptl}) of **3b** of 40.1 % is close to the theoretical value ($SE_{max}=40.8$ %) and is far superior to all other ligands that lack the *t*Bu groups at the phenyl ring (SE_{exptl}: **2a**: 7.7 %, **2b**: 10.9 %, **2c**: 14.9 %; see Table 3).

From the six 1:1 and 1:2 association constants determined by NMR spectroscopic titration (see Table 2 and the Supporting Information), the concentration of each of the six Ni^{2+} complex species can be calculated as a function of the ligand concentration (speciation plots, Figures 4 and 5). At the concentration of **3b** used in the experiment, which was close to the optimal ligand concentration ($[\mathbf{L}]_{opt}$, see Table 3), the predominant complex at PSS-365 in solution is the diamagnetic bare Ni–porphyrin **1** (69 %; Figure 4). At PSS-440, the paramagnetic **1** with two *trans*-**3b** molecules as axial ligands prevails (45 %; Figure 5).

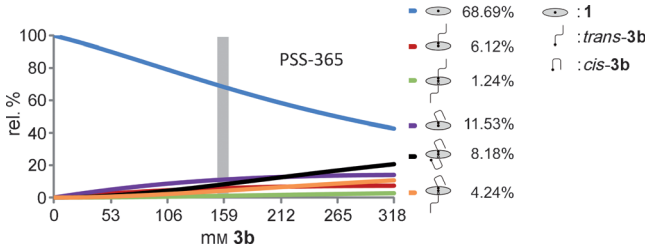

Figure 4. Speciation plot (relative concentrations with respect to $[\mathbf{1}]_{total}$) of **1**, and all axial complexes of **1** as a function of the concentration of **3b**. For **3b**, a ratio of *cis* and *trans* configurations corresponding to PSS-365 was assumed (91 % *cis*, 9 % *trans*). The gray bar indicates the concentration of **3b** (158 mM) at which the switching experiments were performed ($[\mathbf{1}]_{total}=106$ μM). The relative concentrations of all Ni-complex species at this point are given on the right.

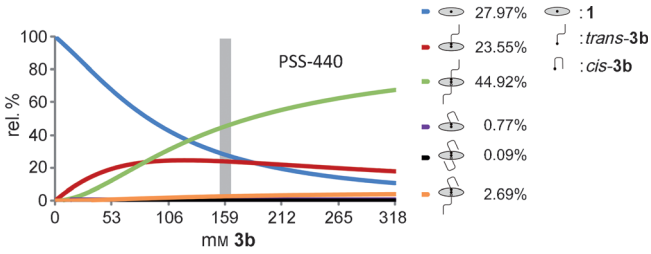

Figure 5. Speciation plot (relative concentrations with respect to $[\mathbf{1}]_{total}$) of **1**, and all axial complexes of **1** as a function of the concentration of **3b**. For **3b**, a ratio of *cis* and *trans* configurations corresponding to PSS-440 was assumed (15 % *cis*, 85 % *trans*). The gray bar indicates the concentration of **3b** (158 mM) at which the switching experiments were performed ($[\mathbf{1}]_{total}=106$ μM). The relative concentrations of all Ni-complex species at this point are given on the right.

According to Equation (5) there is an optimum ligand concentration ($[\mathbf{L}]_{opt}$) for which a maximum switching efficiency (SE_{max}) is attained. Both $[\mathbf{L}]_{opt}$ and SE_{max} are independent of the porphyrin concentration if there is a large excess amount of the ligand ($[\mathbf{L}]_{tot}\approx[\mathbf{L}]$). However, an analytical solution of the problem was only possible for 1:1 complexes. By using the six experimentally determined association constants of **3b** with **1** (Table 2, see the Supporting Information) and a nonlinear treatment of the binding isotherms, we now checked if our assumption that $[\mathbf{L}]_{opt}$ and SE_{max} are independent of the porphyrin concentration were still correct in more complicated systems with mixtures of 1:1 and 1:2 complexes. The results of our simulation (Figure 6) show that in a concentration range from 0 to about 5 mM of **1**, both $[\mathbf{L}]_{opt}$ and SE_{max} are constant. Practical concentrations in switching experiments and the concen-

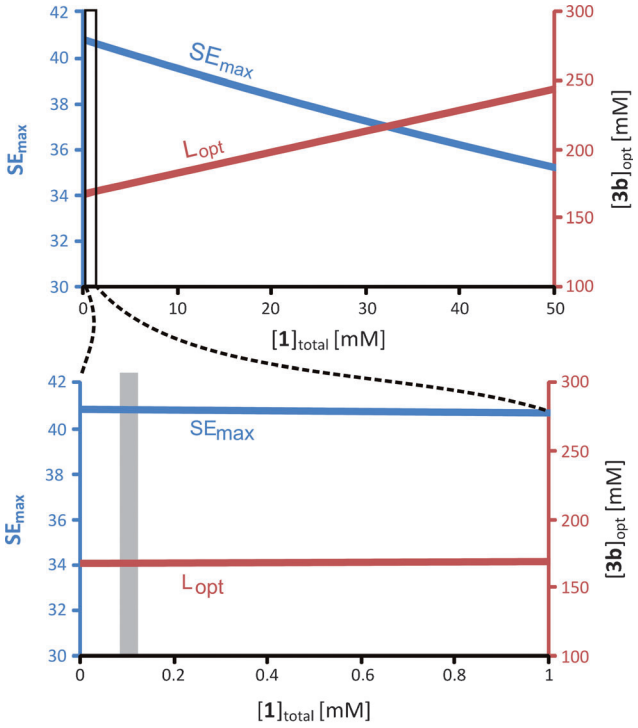

Figure 6. Maximum switching efficiency (SE_{max}; blue curve) and optimal ligand concentration $[\mathbf{L}]_{opt}$ of **3b** as a function of $[\mathbf{1}]_{total}$ (top: 0–50 mM of $[\mathbf{1}]_{total}$). The range with 0–1 mM of $[\mathbf{1}]_{total}$ of the plot is magnified in the bottom figure. SE_{max} and $[\mathbf{L}]_{opt}$ are independent of $[\mathbf{1}]_{total}$ within a range of 0 to 5 mM of $[\mathbf{1}]_{total}$. The gray bar indicates the concentration of $[\mathbf{1}]_{total}$ used in our experiments.

trations used in our experiments are well within this linear range.

Conclusion

Photodissociable ligands (PDLs) are an efficient approach to switch physicochemical properties of metal complexes. The ligands have to be designed in such a way that one configuration binds to the metal complex and the other isomer does not. The maximum attainable switching efficiency (SE_{max}) only depends on the ratio of the association constants of both configurations of the ligand. There is an optimal ligand concentration ($[\mathbf{L}]_{opt}$) that leads to the SE_{max} independent of the concentration of the metal complex. $[\mathbf{L}]_{opt}$ and SE_{max} are system parameters that characterize the combination of a PDL and a metal complex. The strategy that can be derived for the molecular design of a PDL is that more emphasis should be given to reduce the binding of the low-affinity isomer than to optimize the binding properties of its high-affinity counterpart. Effective PDLs based on 3-phenylazopyridine should have both a large substituent at the 4-position of the pyridine ring to disfavor formation of the *cis*-α conformation and two substituents at the 3,5-positions of the phenyl ring are needed to prevent the *cis*-β conformation from binding to the metal complex. A corresponding PDL (**3b**) has been synthesized and successfully tested. Upon irradiation at 365 and 440 nm, a switching efficiency of 40.1% was attained for the reversible conversion of the Ni^{2+} center from high to low spin. Thus, the magnetic susceptibility of the homogeneous solution can be switched by a factor of more than two. Further studies are devoted to the development of stronger binding PDLs that would exhibit SE_{max} at lower concentrations, for example, azoimidazoles.[38]

Experimental Section

General remarks: Solvents and starting materials were used as received. Column chromatography was carried out using 0.04–0.06 mm mesh silica gel from Merck. NMR spectra were recorded at 298 K using a 300 MHz (75.5 MHz for ^{13}C) Bruker ARX 300, 500 MHz (125 MHz for ^{13}C) Bruker DRX 500, or a 600 MHz (150 MHz for ^{13}C) Bruker AV 600. Chemical shifts were calibrated either to the internal standard TMS or using residual protonated solvent signals (^1H ($CHCl_3$): $\delta = 7.24$ ppm, (toluene): $\delta = 2.04$ ppm; and ^{13}C ($CHCl_3$): $\delta = 77.0$ ppm). For the assignment of the NMR spectroscopic signals and the numbering of the corresponding carbon atoms, see the Supporting Information. Mass spectrometry was performed using a Finnigan MAT 8230 (EI, 70 eV) and MAT 8200 (CI, isobutane) instrument. Infrared spectra were recorded using a Perkin–Elmer ATR spectrometer with a Golden-Gate-Diamond-ATR A531-G for neat samples. UV-visible absorption spectra were recorded using a Perkin–Elmer Lambda-14 spectrophotometer with quartz cells of 1 cm path length. All solvents employed in optical spectroscopy were of spectrophotometric grade. Irradiation experiments were performed in toluene. For the isomerization of *trans*- to *cis*-azopyridine, the samples were irradiated using an LED (Nichia NC4U133(T), peak wavelength: (365 ± 9) nm, three LEDs, power dissipation: 12 W each, luminous flux: 10 lm each, distance ≈1 cm). The conversion of *cis*- to *trans*-azopyridine was performed using an LED from Roithner Laser Technik GmbH (VL 440-EMITTER, peak wavelength: (440 ± 5) nm, three LEDs, power dissipation: 1.3 W each, distance ≈1 cm).

Synthesis of starting materials: Nickel–5,10,15,20-tetrakis(pentafluorophenyl)porphyrin (Ni–TPFPP) (**1**) was prepared as described previously.[17]

3-Phenylazopyridine (2a): Prepared by the method of Campbell et al. ^1H and ^{13}C NMR spectroscopic and MS analytical data are consistent with those reported in the literature.[39] *trans* isomer: ^1H NMR (300 MHz, [D_8]toluene, 300 K): $\delta = 9.29$ (d, $J = 2.4$ Hz, 1H; 1-*H*), 8.39 (dd, $J = 4.7$, 1.5 Hz, 1H; 5-*H*), 7.85–7.82 (m, 2H; 7-*H*), 7.76 (ddd, $J = 8.2$, 2.4, 1.7 Hz, 1H; 3-*H*), 7.13–7.08 (m, 3H; 8-*H*, 9-*H*), 6.68 ppm (dd, $J = 8.2$, 4.7 Hz 1H; 4-*H*). *cis* isomer: ^1H NMR (300 MHz, [D_8]toluene, 300 K): $\delta = 8.03$ (d, $J = 2.5$ Hz, 1H; 1-*H*), 8.01 (dd, $J = 4.8$, 1.5 Hz, 1H; 5-*H*), 6.74–6.70 (m, 2H; 8-*H*), 6.66–6.61 (m, 1H; 9-*H*), 6.54 (ddd, $J = 8.1$, 2.5, 1.6 Hz, 1H; 3-*H*), 6.44–6.41 (m, 2H; 7-*H*), 6.36 ppm (ddd, $J = 8.0$, 4.8, 0.8 Hz, 1H; 4-*H*).

4-Methyl-3-(phenylazo)pyridine (2b): 3-Amino-4-methylpyridine (2.29 g, 21.2 mmol), tetramethylammonium hydroxide (57.0 mL, 25%), and pyridine (25 mL) were heated to 80°C. Nitrosobenzene (3.00 g, 28.0 mmol) was dissolved in pyridine (50 mL) and added dropwise. After stirring at 80°C for 45 min. the reaction mixture was allowed to cool down to RT. The crude product was extracted with plenty of toluene. The organic layer was dried over magnesium sulfate and after removal of the solvent, column chromatography on silica gel (cyclohexane, ethyl acetate 1:1, $R_f = 0.58$) afforded a red solid (146 mg, 0.740 mmol, 3%). M.p. 62.8°C; ^1H NMR (600 MHz, $CDCl_3$): $\delta = 8.73$ (s, 1H; 1-*H*), 8.51 (d, $J = 5.0$ Hz, 1H; 5-*H*), 7.93 (dd, $J = 8.2$, 1.6 Hz, 2H; 7-*H*), 7.55–7.48 (m, 3H; 8-*H*, 9-*H*), 7.26 (d, $J = 5.0$ Hz, 1H; 4-*H*), 2.70 ppm (s, 3H; CH_3); ^{13}C NMR (150.9 MHz, $CDCl_3$): $\delta = 152.8$ (*C*-6), 150.8 (*C*-5), 146.5 (*C*-2), 145.2 (*C*-3), 138.0 (*C*-1), 131.5 (*C*-9), 129.1 (*C*-8), 125.9 (*C*-4), 123.1 (*C*-7), 17.1 ppm (CH_3); IR (KBr): $\tilde{\nu} = 3039$ (C–H_{arom}), 2960, 2921 (C–H_{aliph}), 1593, 1466, 1441, (C=C), 833, 769, 726, 688 cm^{-1} (C–H_{def}); MS (EI): *m*/*z*

(%): 197 (49) $[M]^+$, 120 (3) $[M-Ph]^+$, 105 (25) $[PhN_2]^+$, 92 (45) $[M-PhN_2]^+$, 77 (100) $[Ph]^+$; MS (CI): *m/z* (%): 198 (100) $[M+H]^+$; elemental analysis calcd (%) for $C_{12}H_{11}N_3$ (197.26): C 73.07, H 5.62, N 21.30; found: C 73.39, H 5.85, N 21.19. *trans* isomer: ^{1}H NMR (300 MHz, [D$_8$]toluene, 300 K): $\delta = 8.96$ (s, 1H; 1-*H*), 8.31 (d, $J = 4.5$ Hz, 1H; 5-*H*), 7.78 (d, $J = 7.4$ Hz, 2H; 7-*H*), 7.13–7.02 (m, 3H; 8-*H*, 9-*H*), 6.59 (d, $J = 4.8$ Hz, 1H; 4-*H*), 2.28 ppm (s, 3H; CH_3). *cis* isomer: ^{1}H NMR (300 MHz, [D$_8$] toluene, 300 K): $\delta = 7.97$ (d, $J = 5$ Hz, 1H; 5-*H*), 7.49 (s, 1H; 1-*H*), 6.75–6.70 (m, 2H; 8-*H*), 6.66–6.59 (m, 1H; 9-*H*), 6.50–6.48 (m, 2H; 7-*H*), 6.36 (d, $J = 4.5$ Hz, 1H; 4-*H*), 1.85 ppm (s, 3H; CH_3).

4-Isopropyl-3-phenylazopyridine (2c): 2,2-Dimethyl-*n*-(3-pyridyl)propane amide was synthesized by reaction of 3-aminopyridine with trimethylacetyl chloride (64%).[40] A Grignard reaction with isopropyl magnesium chloride led to 2,2-dimethyl-*n*-(4-isopropyl-3-pyridyl)propane amide (46%).[18,41] Deprotection with sulfuric acid gave 3-amino-4-isopropylpyridine (77%).[18] 3-Amino-4-isopropylpyridine (2.00 g, 14.7 mmol), sodium hydroxide (50 mL, 25%), and pyridine (25 mL) were heated to 80°C. Nitrosobenzene (2.04 g, 19.1 mmol) was dissolved in pyridine (50 mL) and added dropwise within 45 min. After stirring at 80°C for 2 h, the reaction mixture was allowed to cool to RT. The crude product was extracted with plenty of toluene. The organic layer was dried over magnesium sulfate, and after removal of the solvent, column chromatography on silica gel (cyclohexane, ethyl acetate 1:1, $R_f = 0.65$) afforded an orange oil (1.20 g, 5.30 mmol, 36%). ^{1}H NMR (500 MHz, $CDCl_3$): $\delta =$ 8.70 (s, 1H; 1-*H*), 8.59 (d, $J = 5.2$ Hz, 1H; 5-*H*), 7.95–7.93 (m, 2H; 9-*H*), 7.52 (m$_c$, 3H; 10-*H*, 11-*H*), 7.36 (dd, $J = 5.2$, 0.4 Hz, 1H; 4-*H*), 3.99 (septet, $J = 7.0$ Hz, 1H; C*H*$(CH_3)_2$), 1.35 ppm (d, $J = 7.0$ Hz, 6H; CH_3); ^{13}C NMR (125.8 MHz, $CDCl_3$): $\delta = 154.9$ (*C*-3), 152.9 (*C*-8), 151.5 (*C*-5), 145.9 (*C*-2), 137.6 (*C*-1), 129.2 (*C*-10), 129.0 (*C*-11), 123.1 (*C*-9), 121.1 (*C*-4), 27.9 (*C*-6), 23.0 ppm (*C*-7); IR (KBr): $\tilde{\nu} = 3052$ (C–H$_{arom}$), 2929, 2870 (C–H$_{aliph}$), 1587, 1466, 1402, (C=C), 833, 757, 686 cm^{-1} (C–H$_{def}$); MS (EI): *m/z* (%): 225 (29) $[M]^+$, 210 (100) $[M-CH_3]^+$, 133 (59) $[M-PhCH_3]^+$, 105 (7) $[PhN_2]^+$; MS (CI): *m/z* (%): 226 (100) $[M+H]^+$, 133 (48) $[M-PhCH_3]^+$; elemental analysis calcd (%) for $C_{14}H_{15}N_3$ (225.13): C 74.64, H 6.71, N 18.65; found: C 74.60, H 6.68, N 19.02. *trans* isomer: ^{1}H NMR (500 MHz, [D$_8$]toluene, 300 K): $\delta = 8.97$ (s, 1H; 1-*H*), 8.44 (d, $J = 5.1$ Hz, 1H; 5-*H*), 7.81–7.78 (m, 2H; 9-*H*), 7.14–7.09 (m, 2H; 10-*H*), 7.07–7.04 (m, 1H; 11-*H*), 6.81 (d, $J = 5.1$ Hz, 1H; 4-*H*), 3.83 (septet, $J = 7.0$ Hz, 1H; C*H*$(CH_3)_2$), 1.07 ppm (d, $J = 7.0$ Hz, 6H; CH_3). *cis* isomer: ^{1}H NMR (500 MHz, [D$_8$]toluene, 300 K): $\delta = 8.08$ (d, $J =$ 5.2 Hz, 1H; 5-*H*), 7.45 (s, 1H; 1-*H*), 6.79–6.74 (m, 2H; 9-*H*), 6.69–6.60 (m, 4H; 4-*H*, 10-*H*, 11-*H*), 3.10 (septet, $J = 6.9$ Hz, 1H; C*H*$(CH_3)_2$), 1.00 ppm (d, $J = 6.9$ Hz, 6H; CH_3).

4-Iodo-3-phenylazopyridine (2d):[42] Lithiation of 2,2-dimethyl-*n*-(3-pyridyl)propane amide and reaction with iodine followed by deprotection of the amine with sulfuric acid afforded 3-amino-4-iodopyridine.[41,43,44] 3-Amino-4-iodopyridine (1.00 g, 4.55 mmol) and nitrosobenzene (490 mg, 4.55 mmol) were dissolved in pyridine (12 mL) and sodium hydroxide (8 mL, 10 N), then stirred at RT for 16 h. The reaction mixture was diluted with water (30 mL) and the organic layer was extracted with toluene. The combined organic layers were dried over magnesium sulfate. After removal of the solvent, purification by column chromatography on silica gel (ethyl acetate, $R_f = 0.59$) afforded a red solid (900 mg, 2.92 mmol, 64%). M.p. 86.1°C; ^{1}H NMR (600 MHz, $CDCl_3$): $\delta = 8.65$ (s, 1H; 1-*H*), 8.21 (d, $J = 5.2$ Hz, 1H; 5-*H*), 8.00 (dd, $J = 7.9$, 1.8 Hz, 2H; 7-*H*), 7.96 (d, $J = 5.2$ Hz, 1H; 4-*H*), 7.56–7.51 ppm (m, 3H; 8-*H*, 9-*H*); ^{13}C NMR (150.9 MHz, $CDCl_3$): $\delta = 152.3$ (*C*-2), 150.9 (*C*-5), 147.4 (*C*-6), 138.7 (*C*-1), 136.6 (*C*-4), 132.2 (*C*-9), 129.3 (*C*-8), 123.7 (*C*-7), 111.5 ppm (*C*-3); IR (KBr): $\tilde{\nu} = 3037$ (C–H$_{arom}$), 1544, 1411, (C=C), 1051 (C–I$_{arom}$), 818, 770, 720, 682 cm^{-1} (C–H$_{def}$); MS (EI): *m/z* (%): 309 (88) $[M]^+$, 204 (24) $[M-PhN_2]^+$, 105 (100) $[PhN_2]^+$; MS (CI): *m/z* (%): 310 (100) $[M+H]^+$, 184 (3) $[M-I+H]^+$, 105 (7) $[PhN_2]^+$; elemental analysis calcd (%) for $C_{11}H_8IN_3$ (309.12): C 42.74, H 2.61, N 13.59; found: C 43.08, H 2.62, N 13.87. *trans* isomer: ^{1}H NMR (300 MHz, [D$_8$]toluene, 300 K): $\delta = 8.64$ (d, $J = 0.5$ Hz, 1H; 1-*H*), 7.87–7.84 (m, 2H; 7-*H*), 7.74 (d, $J = 5.1$ Hz, 1H; 5-*H*), 7.23 (dd, $J = 5.2$ Hz, 0.5 Hz, 1H; 4-*H*), 7.11–7.07 (m, 2H; 8-*H*), 7.05–7.02 ppm (m, 1H; 9-*H*). *cis* isomer: ^{1}H NMR (300 MHz, [D$_8$]toluene, 300 K): $\delta = 7.42$ (d, $J = 5.2$ Hz, 1H; 5-*H*), 7.17 (s, 1H; 1-*H*), 7.02 (d, $J =$ 5.2 Hz, 1H; 4-*H*), 6.72–6.67 (m, 2H; 8-*H*), 6.63–6.61 (m, 1H; 9-*H*), 6.60–6.58 ppm (m, 2H; 7-*H*).

4-Phenyl-3-phenylazopyridine (2e): Prepared by the method of Otsuki et al. ^{1}H NMR and MS analytical data are consistent with those reported in the literature.[23] *trans* isomer: ^{1}H NMR (500 MHz, [D$_8$]toluene, 300 K): $\delta = 9.05$ (d, $J = 0.5$ Hz, 1H; 1-*H*), 8.48 (d, $J = 5.0$ Hz, 1H; 5-*H*), 7.73–7.70 (m, 2H; 7-*H*), 7.22–7.18 (m, 2H; 11-*H*), 7.12–7.07 (m, 3H; 12-*H*, 13-*H*), 7.04–6.98 (m, 3H; 8-*H*, 9-*H*), 6.92 ppm (dd, $J = 5.0$, 0.6 Hz, 1H; 4-*H*). *cis* isomer: ^{1}H NMR (500 MHz, [D$_8$]toluene, 300 K): $\delta = 8.14$ (d, $J = 5.1$ Hz, 1H; 5-*H*), 7.88 (d, $J = 0.6$ Hz, 1H; 1-*H*), 6.69–6.65 (m, 3H), 6.63–6.60 (m, 3H), 6.41–6.38 ppm (m, 2H). Missing signals might have been disguised by signals of the *trans* isomer or the solvent.

3-Amino-4-methoxypyridine:[45] 4-Methoxy-3-nitropyridine (2.00 g, 13.0 mmol) and anhydrous tin(II) chloride (17.3 g, 91.0 mmol) were dissolved in ethanol (50 mL) and acetic acid (7 mL, 2 N) and heated to reflux for 3 h. Ice-cooled water and potassium hydroxide (140 g) were added. The hot layers could be separated and the water layer was extracted with dichloromethane. The combined organic layers were dried over magnesium sulfate. After removal of the solvent, a yellow solid (1.48 g, 11.9 mmol, 92%) was afforded without further purification. M.p. 82°C; ^{1}H NMR (500 MHz, $CDCl_3$): $\delta = 7.99$ (s, 1H; 1-*H*), 7.96 (d, $J =$ 5.4 Hz, 1H; 5-*H*), 6.68 (d, $J = 5.4$ Hz, 1H; 4-*H*), 3.88 (s, 3H; CH_3), 3.72 ppm (br s, 2H; NH_2); ^{13}C NMR (125.8 MHz, $CDCl_3$): $\delta = 152.9$ (*C*-3), 141.6 (*C*-1), 136.5 (*C*-5), 132.8 (*C*-2), 105.5 (*C*-4), 55.3 ppm (*C*H$_3$); IR (KBr): $\tilde{\nu} = 3401$, 3331 (N–H), 3166, 3089 (C–H$_{arom}$), 2999, 2935 (C–H$_{aliph}$), 1574, 1511, 1426, (C=C), 1232, 1025, 856, 806, 767 cm^{-1} (C–H$_{def}$); MS (EI): *m/z* (%): 124 (100) $[M]^+$, 109 (35) $[M-CH_3]^+$; MS (CI): *m/z* (%): 125 (100) $[M+H]^+$; elemental analysis calcd (%) for $C_6H_8N_2O$ (124.06): C 58.05, H 6.50, N 22.57; found: C 57.91, H 6.63, N 21.59.

4-Methoxy-3-phenylazopyridine (2f): 3-Amino-4-methoxypyridine (1.00 g, 8.06 mmol) was dissolved in pyridine (4.00 mL) and sodium hydroxide (6.00 mL, 75.0 mmol, 25%) and heated to 80°C. Within 45 min, nitrosobenzene (1.15 g, 15.8 mmol) dissolved in pyridine (30 mL) was added dropwise. The reaction mixture was stirred at 80°C for an additional 45 min. After cooling, the water layer was extracted with toluene and dried over magnesium sulfate. After removal of the solvent, purification by column chromatography on silica gel (ethyl acetate/triethylamine (5%), $R_f = 0.4$) and recrystallization from diethyl ether afforded red crystals (611 mg, 2.87 mmol, 36%). M.p. 80.4°C; ^{1}H NMR (500 MHz, $CDCl_3$): $\delta = 8.66$ (s, 1H; 1-*H*), 8.54 (d, $J = 5.8$ Hz, 1H; 5-*H*), 7.91 (m, 2H; 7-*H*), 7.50 (m, 3H; 8-*H*, 9-*H*), 4.01 ppm (s, 3H; CH_3); ^{13}C NMR (150.9 MHz, $CDCl_3$): $\delta = 161.8$ (*C*-3), 153.0 (*C*-5), 152.97 (*C*-2), 139.1 (*C*-1), 138.3 (*C*-6), 134.4 (*C*-9), 129.2 (*C*-8), 123.1 (*C*-7), 107.9 (*C*-4), 56.2 ppm (*C*H$_3$); IR (KBr): $\tilde{\nu} = 1582$, 1567, 1491, 1439, 1470 (C=C), 1016, 812 cm^{-1} (C–H$_{def}$); MS (EI): *m/z* (%): 213 (100) $[M]^+$, 105 (57) $[M-C_6H_6NO]^+$; MS (CI): *m/z* (%): 214 (100) $[M+H]^+$; elemental analysis calcd (%) for $C_{12}H_{11}N_3O$ (213.09): C 67.59, H 5.20, N 19.71; found: C 67.44, H 5.32, N 19.56. *trans* isomer: ^{1}H NMR (300 MHz, [D$_8$]toluene, 300 K): $\delta = 8.91$ (s, 1H; 1-*H*), 8.28 (d, $J = 5.7$ Hz, 1H; 5-*H*), 7.91–7.86 (m, 2H; 7-*H*), 7.00–7.10 (m, 3H; 8-*H*, 9-*H*), 5.73 (d, $J = 5.7$ Hz, 1H; 4-*H*), 3.18 ppm (s, 3H; OCH_3); *cis* isomer: ^{1}H NMR (300 MHz, [D$_8$]toluene, 300 K): $\delta = 7.99$ (d, $J = 5.6$ Hz, 1H; 5-*H*), 7.84 (s, 1H; 1-*H*), 6.78–6.71 (m, 2H; 7-*H*), 6.68–6.59 (m, 3H; 8-*H*, 9-*H*), 5.83 (d, $J = 5.6$ Hz, 1H; 4-*H*), 2.83 ppm (s, 3H; OCH_3).

4-*N,N*-Dimethylamino(3-phenylazo)pyridine (2g): Prepared by the reduction of 3-nitro-4-dimethylaminopyridine and reaction of the amine with nitrosobenzene. ^{1}H and ^{13}C NMR spectroscopy and MS analytical data are consistent with those reported in the literature.[23] *trans* isomer: ^{1}H NMR (600 MHz, [D$_8$]toluene, 300 K): $\delta = 8.93$ (s, 1H; 1-*H*), 8.17 (d, $J = 6.0$ Hz, 1H; 5-*H*), 7.73 (m$_c$, 2H; 7-*H*), 7.13 (m$_c$, 3H; 8-*H*, 9-*H*), 6.11 (d, $J = 6.0$ Hz, 1H; 4-*H*), 2.58 ppm (s, 6H; N$(CH_3)_2$). *cis* isomer: ^{1}H NMR (600 MHz, [D$_8$]toluene, 300 K): $\delta = 7.89$ (d, $J = 5.8$ Hz, 1H; 5-*H*), 7.41 (s, 1H; 1-*H*), 6.83–6.79 (m, 2H; 7-*H*), 6.74–6.65 (m, 3H; 8-*H*, 9-*H*), 5.94 (d, $J = 5.8$ Hz, 1H; 4-*H*), 2.43 ppm (s, 6H; N$(CH_3)_2$).

4-Methyl-3(3′,5′di-*tert*-butylphenyl)azopyridine (3b): A solution of Oxone (6.00 g, 9.76 mmol) in water (50 mL) was added to a solution of 3,5-di-*tert*-butylaniline (1.00 g, 4.88 mmol) in dichloromethane (20 mL). After stirring for 4 h at room temperature, the layers were separated.

The aqueous layer was extracted twice with dichloromethane. The combined organic layers were dried over magnesium sulfate. After removal of the solvent, column chromatography on silica gel (CH_2Cl_2, $R_f = 0.3$ pale green fraction) afforded a green solid assigned as 3,5-di-*tert*-butylnitrosobenzene (851 mg, 3.89 mmol, 80%). ^{1}H NMR (500 MHz, $CDCl_3$): $\delta = 7.83$ (t, $J = 1.9$ Hz, 1H; 4-*H*), 7.78 (d, $J = 1.9$ Hz, 2H; 2-*H*), 1.40 ppm (s, 18H; CH_3); ^{13}C NMR (125.8 MHz, $CDCl_3$): $\delta = 167.1$ (*C*-1), 152.4 (*C*-3), 129.7 (*C*-2), 115.9 (*C*-4), 35.1 ($C(CH_3)_3$), 31.2 ppm ($C(CH_3)_3$); IR (KBr): $\tilde{\nu} = 2962$ (C–H_{arom}), 2904, 2869 (C–H_{aliph}), 1597, 1535, 1478, 1460, 1449 (C=C), 1363, 1312, 1246, 885, 699 cm^{-1} (C–H_{def}); MS (EI): *m*/*z* (%): 219 (66) $[M]^+$, 189 (92) $[M-NO]^+$, 133 (100) $[M-NO-t\mathrm{Bu}]^+$; MS (CI): *m*/*z* (%): 220 (100) $[M+H]^+$.

3-Amino-4-methylpyridine (378 mg, 3 mmol) was dissolved in pyridine (5 mL) and 60% potassium hydroxide (15 mL) and was heated to 100°C. A solution of 3,5-di-*tert*-butylnitrosobenzene (851 mg, 3.89 mmol) in pyridine (25 mL) was added dropwise. After stirring for 16 h, the reaction mixture was allowed to cool, and the layers were separated. The aqueous layer was extracted once with toluene (100 mL) and twice with toluene (40 mL). The combined organic layers were dried over magnesium sulfate. After removal of the solvent, column chromatography on silica gel (cyclohexane, ethyl acetate 2:1, $R_f = 0.5$) afforded an orange oil (95.1 mg, 0.310 mmol, 9%). ^{1}H NMR (500 MHz, $CDCl_3$): $\delta = 8.69$ (s, 1H; 1-*H*), 8.50 (d, $J = 5.0$ Hz, 1H; 5-*H*), 7.79 (d, $J = 1.8$ Hz, 2H; 8-*H*), 7.60 (t, $J = 1.8$ Hz, 1H; 10-*H*), 7.27 (d, $J = 5.0$ Hz, 1H; 4-*H*), 2.69 (s, 3H; CH_3), 1.40 ppm (s, 18H; C(CH_3)$_3$); ^{13}C NMR (125.8 MHz, $CDCl_3$): $\delta = 152.0$ (*C*-1), 152.4 (*C*-3), 129.7 (*C*-2), 115.9 (*C*-4), 35.1 ($C(CH_3)_3$), 31.2 ppm (C-(CH_3)$_3$); IR (KBr): $\tilde{\nu} = 3057$, 2960 (C–H_{arom}), 2905, 2868 (C–H_{aliph}), 1592, 1478, 1461, 1439, 1394 (C=C), 1363, 1246, 1154, 900, 885, 824, 731, 699 cm^{-1} (C–H_{def}); MS (EI): *m*/*z* (%): 309 (44) $[M]^+$, 189 (100) $[M-NN-Py]^+$; MS (CI): *m*/*z* (%): 310 (100) $[M+H]^+$. *trans* isomer: ^{1}H NMR (500 MHz, [D$_8$]toluene, 300 K): $\delta = 9.03$ (s, 1H; 1-*H*), 8.33 (d, $J = 5.0$ Hz, 1H; 5-*H*), 7.93 (d, $J = 1.9$ Hz, 2H; 8-*H*), 7.57 (t, $J = 1.8$ Hz, 1H; 10-*H*), 6.62 (d, $J = 5.0$ Hz, 1H; 4-*H*), 2.35 (s, 3H; CH_3), 1.25 ppm (s, 18H; C(CH_3)$_3$). *cis* isomer: ^{1}H NMR (500 MHz, [D$_8$]toluene, 300 K): $\delta = 7.98$ (d, $J = 4.9$ Hz, 1H; 5-*H*), 7.56 (s, 1H; 1-*H*), 7.15 (t, $J = 1.7$ Hz, 1H; 10-*H*), 6.67 (d, $J = 1.7$ Hz, 2H; 8-*H*), 6.41 (d, $J = 5.0$ Hz, 1H; 4-*H*), 1.88 (s, 3H; CH_3), 1.00 ppm (s, 18H; C(CH_3)$_3$).

Acknowledgements

We gratefully acknowledge support by the Deutsche Forschungsgemeinschaft through SFB 677 (Function by Switching).

[1] O. Kahn, *Molecular Magnetism*, Wiley-VCH, New York, **1993**.
[2] *Dalton Trans.* **2010**, *39*, 4671, themed issue on "Molecular Magnets".
[3] R. N. Muller, L. V. Elst, S. Laurent, *J. Am. Chem. Soc.* **2003**, *125*, 8405–7.
[4] C. Tu, E. A. Osborne, A. Y. Louie, *Tetrahedron* **2009**, *65*, 1241–1246.
[5] C. Rajadurai, M. Ruben, D. Kruk, WO 2009/080138A2.
[6] F. Touti, P. Maurin, L. Canaple, O. Beuf, J. Hasserodt, *Inorg. Chem.* **2012**, *51*, 31–33.
[7] U. Andres, *Magnetohydrodynamic and Magnetohydrostatic Methods of Mineral Separation*, Wiley, New York, **1976**.
[8] K. A. Mirica, S. S. Shevkoplyas, S. T. Phillips, M. Gupta, G. M. Whitesides, *J. Am. Chem. Soc.* **2009**, *131*, 10049–10058.
[9] *J. Mater. Chem.* **2009**, *19*, 1670–1695 themed issue on "Molecular Spintronics and Quantum Computing".
[10] C. Roux, J. Zarembowitch, B. Gallois, T. Garnier, R. Claude, *Inorg. Chem.* **1994**, *33*, 2273–2279.
[11] M.-L. Boillot, C. Roux, J.-P. Audiére, A. Dausse, J. Zarembowitch, *Inorg. Chem.* **1996**, *35*, 3975–3980.
[12] M.-L. Boillot, S. Chantrine, J. Zarembowitch, J. Y. Lallemond, J. Prunet, *New J. Chem.* **1999**, *23*, 179–184.
[13] Y. Hasegawa, S. Kume, H. Nishihara, *Dalton Trans.* **2009**, 280–284.
[14] M. M. Paquette, B. O. Patrick, N. L. Frank, *J. Am. Chem. Soc.* **2011**, *133*, 10081–10093.
[15] M. M. Paquette, R. A. Kopelman, E. Beitler, N. L. Frank, *Chem. Commun.* **2009**, 5424–5426.
[16] For a review on the switching of magnetic properties through external stimuli, see: O. Sato, J. Tao, Y.-Z. Zhang, *Angew. Chem.* **2007**, *119*, 2200–2236; *Angew. Chem. Int. Ed.* **2007**, *46*, 2152–2187.
[17] S. Thies, C. Bornholdt, F. Köhler, F. D. Sönnichsen, C. Näther, F. Tuczek, R. Herges, *Chem. Eur. J.* **2010**, *16*, 10074–10083.
[18] S. Thies, H. Sell, C. Schütt, C. Bornholdt, C. Naether, F. Tuczek, R. Herges, *J. Am. Chem. Soc.* **2011**, *133*, 16243–16250.
[19] S. Venkataramani, U. Jana, M. Dommaschk, F. D. Sönnichsen, F. Tuczek, R. Herges, *Science* **2011**, *331*, 445–448.
[20] F. A. Cotton, G. Wilkinson, C. A. Murillo, M. Bochmann, *Advanced Inorganic Chemistry*, Wiley Interscience, New York, **1999**, 6th ed..
[21] M. Schmittel, S. De, S. Pramanik, *Angew. Chem.* **2012**, *124*, 3898–3902; *Angew. Chem. Int. Ed.* **2012**, *51*, 3832–3836.
[22] J. Otsuki, K. Narutaki, J. M. Bakke, *Chem. Lett.* **2004**, *33*, 356–357.
[23] J. Otsuki, N. Narutaki, *Bull. Chem. Soc. Jpn.* **2004**, *77*, 1537–1544.
[24] J. Otsuki, T. Akasaka, K. Araki, *Coord. Chem. Rev.* **2008**, *252*, 32–56.
[25] K. Suwa, J. Otsuki, K. Goto, *Tetrahedron Lett.* **2009**, *50*, 2106–2108.
[26] C. Bornholdt, *Dissertation*, CAU Kiel, **2008**.
[27] G. Füchsel, T. Klammroth, J. Dokić, P. Saalfrank, *J. Phys. Chem. B* **2006**, *110*, 16337–16345.
[28] J. P. Perdew, K. Burke, Y. Wang, *Phys. Rev. B* **1996**, *54*, 16533–39.
[29] A. Schäfer, C. Huber, R. Ahlrichs, *J. Chem. Phys.* **1994**, *100*, 5829–5835.
[30] The *trans*/*cis* percentage was determined by integration of the ^{1}H NMR spectroscopic signals of the 4-*H* (**2a**), 4-methyl (**2b**), the C*H*Me$_2$ proton of the 4-isopropyl group (**2c**), the 4-methoxy group (**2f**), and the NMe$_2$ group (**2g**). In the case of **2d** and **2e**, we used the 5-*H* of the pyridine ring, and in the case of **3b** the 4-methyl protons were integrated to determine the *trans*/*cis* percentage.
[31] F. A. Walker, E. Hui, J. M. Walker, *J. Am. Chem. Soc.* **1975**, *97*, 2390–2397.
[32] C. Frassineti, S. Ghelli, P. Gans, A. Sabatini, M. S. Moruzzi, A. Vacca, *Anal. Biochem.* **1995**, *231*, 374–382.
[33] S. del Piero, A. Melchior, P. Polese, R. Portanova, M. Tolazzi, *Ann. Chim.* **2006**, *96*, 29–49.
[34] TURBOMOLE, version 6.0, R. Ahlrichs, Universität Karlsruhe (Germany), **2009**, see http://www.turbomole.com.
[35] S. F. Boys, F. Bernardi, *Mol. Phys.* **1970**, *19*, 553.
[36] S. Simon, M. Duran, J. J. Dannenberg, *J. Chem. Phys.* **1996**, *105*, 11024–11031.
[37] T. Helgaker, W. Klopper, H. Koch, J. Noga, *J. Chem. Phys.* **1997**, *106*, 9639–9646.
[38] T. Wendler, C. Schuett, C. Naether, R. Herges, *J. Org. Chem.* **2012**, *77*, 3284–3287.
[39] N. Campbell, A. W. Henderson, D. Taylor, *J. Chem. Soc.* **1953**, 1281–1285.
[40] J. A. Turner, *J. Org. Chem.* **1983**, *48*, 3401–3408.
[41] V. Bonnet, F. Mongin, F. Trécourt, G. Quéguiner, *J. Chem. Soc. Perkin Trans. 1* **2000**, 4245–4249.
[42] A. Modrow, D. Zargarani, R. Herges, N. Stock, *Dalton Trans.* **2011**, *40*, 4217–4222.
[43] J. Malm, B. Rehn, A.-B. Hörnfeldt, S. Gronowitz, *J. Heterocycl. Chem.* **1994**, *31*, 11–15.
[44] L. Estel, F. Marsais, G. Quéguiner, *J. Org. Chem.* **1988**, *53*, 2740–2744.
[45] T. Wieland, C. Fest, G. Pfleiderer, *Justus Liebigs Ann. Chem.* **1961**, *642*, 163.

Received: May 14, 2012
Revised: August 29, 2012
Published online: October 22, 2012

